Developmental Biology 334 (2009) 535–546

Contents lists available at ScienceDirect

Developmental Biology

journal homepage: www.elsevier.com/developmentalbiology

Genomes & Developmental Control

Two Hox cofactors, the Meis/Hth homolog UNC-62 and the Pbx/Exd homolog CEH-20, function together during *C. elegans* postembryonic mesodermal development

Yuan Jiang, Herong Shi, Jun Liu *

Department of Molecular Biology and Genetics, Cornell University, 439 Biotechnology Building, Ithaca, NY 14853, USA

ARTICLE INFO

Article history:
Received for publication 5 May 2009
Revised 14 July 2009
Accepted 20 July 2009
Available online 28 July 2009

Keywords:
Meis
Hth
unc-62
Pbx
Exd
ceh-20
Hox
C. elegans
Mesoderm

ABSTRACT

The TALE homeodomain-containing PBC and MEIS proteins play multiple roles during metazoan development. Mutations in these proteins can cause various disorders, including cancer. In this study, we examined the roles of MEIS proteins in mesoderm development in *C. elegans* using the postembryonic mesodermal M lineage as a model system. We found that the MEIS protein UNC-62 plays essential roles in regulating cell fate specification and differentiation in the M lineage. Furthermore, UNC-62 appears to function together with the PBC protein CEH-20 in regulating these processes. Both *unc-62* and *ceh-20* have overlapping expression patterns within and outside of the M lineage, and they share physical and regulatory interactions. In particular, we found that *ceh-20* is genetically required for the promoter activity of *unc-62*, providing evidence for another layer of regulatory interactions between MEIS and PBC proteins.

Introduction

Hox genes encode homeodomain (HD)-containing proteins that establish body plan and specify cell fates during embryogenesis and organogenesis (McGinnis and Krumlauf, 1992; Krumlauf, 1994; Pearson et al., 2005). As monomers, Hox proteins bind to DNA with poor selectivity and affinity *in vitro*. However, interactions with other DNA-binding proteins can increase the DNA-binding specificity and affinity of Hox proteins *in vitro* and therefore facilitate Hox proteins to bind distinct *in vivo* biological targets. Several members of the TALE (*T*hree-*A*mino-*A*cid *L*oop *E*xtension) class of homeodomain proteins can function as Hox partners to modulate Hox-dependent transactivation in invertebrates and vertebrates (Mann and Affolter, 1998; Moens and Selleri, 2006). These Hox cofactors are further grouped into PBC and MEIS classes based on the additional motifs located N-terminal to the homeodomain (Burglin, 1997, 1998; Mukherjee and Burglin, 2007).

The PBC class of homeodomain proteins is represented by the vertebrate Pbx proteins and the *Drosophila* Extradenticle (Exd) protein (Bürglin and Ruvkun, 1992; Rauskolb et al., 1993; Burglin, 1997, 1998; Mukherjee and Burglin, 2007). In addition to the homeodomain, this class of proteins contains two other conserved domains, PBC-A and PBC-B, and the PBC-A domain mediates the interaction of PBC proteins with the MEIS subfamily of proteins (Chang et al., 1997; Knoepfler et al., 1997). The MEIS class of homeodomain proteins includes the vertebrate Meis and Prep1 proteins and the *Drosophila* Homothorax (Hth) protein (Burglin, 1997, 1998; Mukherjee and Burglin, 2007). Recent studies found that both Hth and Meis1 encode two types of isoforms, one HD-containing and one HD-less (Noro et al., 2006). All MEIS proteins share two domains at their N-termini: HM1 and HM2 (also referred to as MEIS A and MEIS B), which are essential for mediating interactions between MEIS and PBC proteins (Rieckhof et al., 1997; Ryoo et al., 1999, Burglin, 1997, 1998; Mukherjee and Burglin, 2007).

PBC and MEIS proteins primarily modulate Hox functions by forming hetero-dimeric or trimeric complexes with Hox proteins on DNA (for examples, see Maconochie et al., 1997; Kroon et al., 1998; Swift et al., 1998; Ryoo et al., 1999; Shanmugam et al., 1999; Shen et al., 1999; Ferretti et al., 2000; Ebner et al., 2005). In these complexes, the PBC or MEIS proteins either directly bind DNA or serve as non-DNA-binding partners to stabilize the complex. PBC and MEIS can also form stable heterodimers with each other in the presence or absence of DNA (Chang et al., 1997; Rieckhof et al., 1997; Abu-Shaar et al., 1999; Berthelsen et al., 1999; Jaw et al., 2000). In addition to their physical interaction, PBC and MEIS proteins also display mutual regulatory interactions. A number of studies have shown that MEIS proteins are required for the nuclear localization and stability of PBC

* Corresponding author. Fax: +1 607 255 6249.
E-mail address: JL53@cornell.edu (J. Liu).

0012-1606/$ – see front matter © 2009 Elsevier Inc. All rights reserved.
doi:10.1016/j.ydbio.2009.07.034

proteins (Pai et al., 1998; Abu-Shaar et al., 1999; Affolter et al., 1999; Berthelsen et al., 1999; Kurant et al., 1998; Stevens and Mann, 2007). Work in *Drosophila* showed that in *exd* mutants, HTH protein levels are undetectable in the developing brain and epidermis and greatly reduced in multiple other embryonic tissues, suggesting that the maintenance of HTH protein level is dependent on EXD activity (Kurant et al., 1998; Nagao et al., 2000).

C. elegans contains both PBC and MEIS proteins. CEH-20 and two divergent members, CEH-40 and CEH-60, comprise the PBC class (Burglin, 1997, 1998; Van Auken et al., 2002; Mukherjee and Burglin, 2007). UNC-62 is the HD-containing MEIS1/hth ortholog, while PSA-3 is a HD-less variant of the PREP family that belongs to the ancient MEIS class (Burglin, 1997; Van Auken et al., 2002; Arata et al., 2006; Mukherjee and Burglin, 2007). A number of studies have shown that Hox and CEH-20 function in a complex to directly regulate downstream gene expression during mesodermal and vulval development, and in regulating apoptosis (Liu and Fire, 2000; Koh et al., 2002; Shemer and Podbilewicz, 2002; Liu et al., 2006; Takacs-Vellai et al., 2007; Potts et al., 2009). However, the roles of MEIS proteins and their functional interactions with Hox and PBC proteins in *C. elegans* are not well characterized. *unc-62* has been shown to function during embryogenesis, Q neuroblast migration, vulval formation and VC motor neuron survival (Van Auken et al., 2002; Yang et al., 2005; Potts et al., 2009). While *unc-62* interacts genetically with *ceh-20* and *ceh-40* during embryogenesis, these genes do not appear to function together with any of the Hox genes (Van Auken et al., 2002). Similarly, loss of *unc-62* or *ceh-20* activity causes Q cell migration and vulval formation defects different than those seen upon loss of Hox activity, suggesting that UNC-62 and CEH-20 may function independently of Hox proteins in regulating these processes (Yang et al., 2005). Finally, the HD-less protein PSA-3 appears to function as a non-DNA-binding partner of CEH-20 and the Hox protein NOB-1 in regulating T cell asymmetric cell division (Arata et al., 2006).

We use the *C. elegans* postembryonic mesodermal lineage, the M lineage, as a model system to investigate the roles of MEIS proteins and their relationships with PBC and Hox proteins during mesodermal development. The *C. elegans* M lineage originates from a single embryonic pluripotent precursor, the M mesoblast (Sulston and Horvitz, 1977). At the first larval stage (L1) in hermaphrodites, the M lineage undergoes four to five rounds of cell division and produces 18 descendants, including two non-muscle coelomocytes (CCs), 14 striated bodywall muscles (BWMs) and two sex myoblasts (SMs) (Fig. 1A). The two SMs migrate from the posterior to the presumptive vulval region and during the L3 stage divide three times to generate 16 precursor cells that eventually differentiate into four classes of non-striated sex muscles required for egg-laying: type I and II vulval muscles (VM1 and VM2) and type I and II uterine muscles (UM1 and UM2). Vulval muscles form tubular muscles and attach to the vulva, while uterine muscles ingress, form thin sheets and attach to the uterus (Sulston and Horvitz, 1977).

Previous studies have shown that two medial group Hox genes, *mab-5* and *lin-39*, share redundant roles in the M lineage, and that they function together with the Hox cofactor *ceh-20* in regulating the specification and diversification of the M lineage (Liu and Fire, 2000). One of the direct target genes of the Hox/CEH-20 complex is the *hlh-8* gene, which encodes the *C. elegans* Twist ortholog and is expressed in all undifferentiated cells in the M lineage (Harfe et al., 1998; Liu and Fire, 2000). The homeobox gene *mls-2* is likely another direct target of CEH-20, although the activation of *mls-2* by CEH-20 appears to be Hox-independent (Jiang et al., 2005, 2008).

In this study, we set out to determine the functions of MEIS proteins in M lineage development. We showed that while *psa-3* does not have an apparent role in the M lineage, *unc-62* has multiple functions throughout M lineage development. Furthermore, *unc-62* genetically interacts with *ceh-20* and *mab-5* to regulate the expression of downstream target genes such as *hlh-8*. Finally, we provide evidence that *unc-62* and *ceh-20* can bind to each other in the yeast two-hybrid system and that they exhibit mutual regulatory interactions: while *unc-62* is required for the nuclear accumulation of CEH-20, *ceh-20* is required for the promoter activity of *unc-62*.

Materials and methods

C. elegans strains

Strains were manipulated under standard conditions as described by Brenner (1974). Analyses were performed at 20 °C, unless otherwise noted. The wild-type reference strain was LW0081 *[ccIs4438 (intrinsic CC::gfp) III; ayIs2 (egl-15::gfp) IV; ayIs6 (hlh-8::gfp) X]* (Jiang et al., 2005). Other M lineage-specific reporters, including *Nde-box::gfp*, *arg-1::gfp*, *rgs-2::gfp* and *mls-2::lacZ*, were as described in Kostas and Fire (2002). The mutant alleles used in this work are: LGIII, *ceh-20(ay9, ay42, n2513, ok541, os39, os114)*, *unc-36(e251)* and *unc-119(ed3)*; LGV, *unc-62(e917, e644, ku234)*, *dpy-11(e224)* and *him-5(e1467)*; LGX, *psa-3(os8)*.

RNA interference

Plasmids to make dsRNA are: p15.121A (Wang et al., 1993) for *lin-39*, pJKL422.1 (Liu and Fire, 2000) for *ceh-20*, and *yk414a1* (gift from Yuji Kohara, National Institute of Genetics, Japan) for *unc-62*. For *mab-5* RNAi, primers JKL-601 and JKL-602 were used to amplify the insert in the *mab-5* RNAi clone III-4I09 from the Ahringer library (Kamath et al., 2003). dsRNA synthesis was following the protocol of Fire et al. (1998). For *ceh-20*, *mab-5* or *lin-39* RNAi, dsRNA was injected into gravid adults of different genotypes. Progeny of injected animals were scored for M lineage and vulval defects. Water-injected animals were used as controls. RNAi soaking was used for *unc-62 (RNAi-soaking)* by modifying the soaking protocol described in Ahringer (2006). Embryos and the subsequent newly hatched L1s were soaked in dsRNA against *unc-62* or in soaking buffer alone for 24–48 h at 20 °C. The soaked L1 worms were transferred to NGM plates with OP50 and followed through development for M lineage phenotypes or *gfp* expression.

Transgenic animals and mls-1::lacZ expression

2.9 kb of the *unc-62* promoter sequence (−2883 to −1 exon 1a) were amplified using iProof DNA polymerase (Bio-Rad Laboratories) using genomic DNA as template and YJ-178 and YJ-179 as primers. The PCR products were used to generate a reporter construct, pYJ167 (−2.9 kb *unc-62p::gfp::let-858* 3′ UTR). pJKL790 and pJKL791 are *unc-62* rescuing constructs that contain the *unc-62* promoter driving *unc-62* 1a–7b and *unc-62* 1b–7b cDNAs respectively.

pHK110 (a gift from Thomas Burglin, Karolinska Institutet, Sweden) and pJKL775 were used for analyzing the *ceh-20* expression pattern. pHK110 contains 2.4 kb of the *ceh-20* promoter sequence (−2385 to −1), the entire *ceh-20* coding region fused with the *gfp* sequence at the C-terminus, and the *unc-54* 3′ UTR. pJKL775 is a transcriptional reporter of *ceh-20* with *nls::gfp* under the control of the *ceh-20* promoter (−2385 to −1).

Reporters were microinjected with the plasmid pRF4 (Mello et al., 1991) or the *pha-1* rescuing plasmid pC1 (Granato et al., 1994) as markers using standard techniques. LW1175 was a spontaneous integrant of pHK110. pSAK534 (*mls-1::lacZ*) (Kostas and Fire, 2002) was microinjected with pRF4 and pJKL449.1 (*myo-2::gfp*) into N2 worms using standard techniques (Mello et al., 1991). Animals transgenic for *jjEx[pSAK534.1(mls-1::lacZ)+rol-6(su1006)+ pJKL449.1(myo-2::gfp)]* were crossed to animals of *unc-62(ku234)*V; *ayIs6 (hlh-8::gfp) X* to generate *unc-62(ku234)*V; *ayIs6 (hlh-8::gfp) X; jjEx[pSAK534.1(mls-1::lacZ)+rol-6(su1006)+ pJKL449.1(myo-2::gfp)]* animals. L3 larvae were fixed following the protocol of Harfe et al.

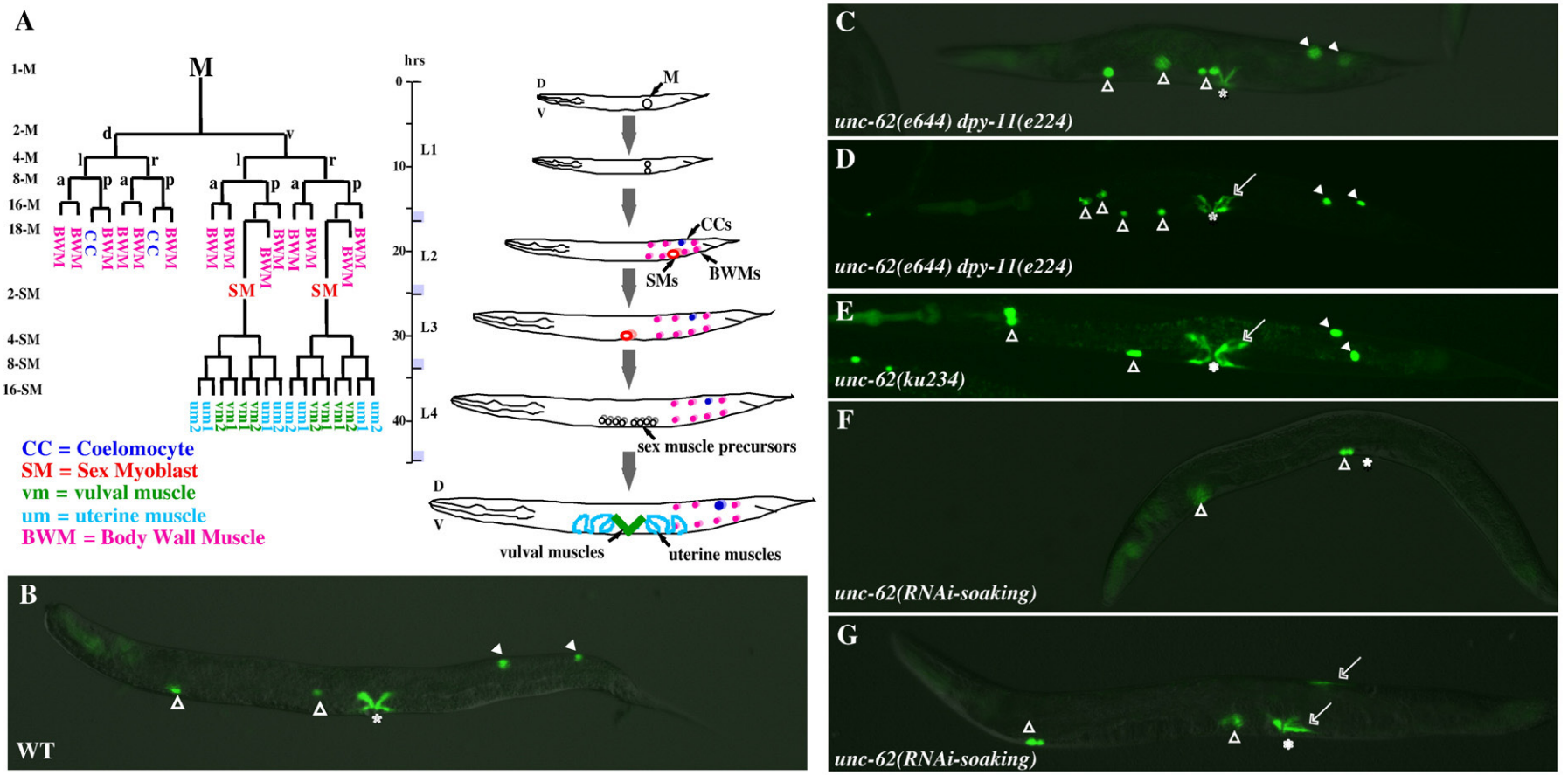

Fig. 1. *unc-62* is required for proper development of the M lineage. (A) The *C. elegans* hermaphrodite postembryonic M lineage. Times are indicated post-hatching at 25 °C. The M lineage showing all differentiated cell types is shown on the left (modified from Sulston and Horvitz, 1977), while a schematic lateral view of the M lineage through larval development is shown on the right. The different stages of the M lineage are also depicted as 1-M through 16-SM. D, dorsal; V, ventral; L, left; R, right; A, anterior; P, posterior. (B–H) Wild-type (B), *unc-62(e644) dpy-11(e224)* (C, D), *unc-62(ku234)*, and *unc-62(RNAi-soaking)* (F, G) adult animals visualized using an *intrinsic CC*::*gfp* and *egl-15*::*gfp*. Open arrowheads point to embryonic CCs, while solid arrowheads point to M-derived CCs. Arrows point to either extra type I vulval muscles (VM1s) in the vulval region (the vulva is denoted by an asterisk) or ectopic *egl-15*::*gfp*-positive cells in the posterior. (C) A *unc-62(e644) dpy-11(e224)* animal with normal numbers of CCs and VM1s. (D) A *unc-62(e644) dpy-11(e224)* animal with normal numbers of CCs but extra VM1s. (E) A *unc-62(ku234)* animal with normal numbers of CCs but extra VM1s. (F) A *unc-62(RNAi-soaking)* animal with no M-derived CCs and VM1s. (G) A *unc-62(RNAi-soaking)* animal with no M-derived CCs and extra VM1-like cells located both in the vulval region and on the dorsal side of the animal.

(1998) and used for immunostaining. The following antibodies were used: goat anti-GFP antibodies (Rockland Immunochemicals) (1:5000), mouse anti-β-galactosidase antibodies (Promega) (1:50), Cy3-conjugated donkey anti-mouse antibodies (Jackson Immunoresearch Laboratories) (1:100) and FITC-conjugated donkey anti-goat antibodies (Jackson Immunoresearch Laboratories) (1:100).

Yeast two-hybrid assay

Two-hybrid analysis was performed using the protocol described by James et al. (1996). The following plasmids were used in the two-hybrid assay:

pYJ188: *ceh-20* aa1–196 in pGAD-C2
pJKL841: *ceh-20* aa1–196 in pGBD-C2
pJKL842: *unc-62* isoform 1a7b aa1–287 in pGBD-C2
pJKL843: *unc-62* isoform 1a7b aa1–287 in pGAD-C2
pJKL844: *unc-62* isoform 1b7b aa1–250 in pGAD-C1
pJKL845: *unc-62* isoform 1b7b aa1–250 in pGBD-C1

Plasmids were transformed into the yeast strain PJ69-4A and selected for on -Trp (pYJ188, pJKL843 and pJKL844) or -Leu (pJKL841, pJKL842 and pJKL845) plates. Transformed strains were tested for auto-activation (growth) on -Ade plates. Transformed yeast colonies were mated in liquid culture and plated in serial dilutions on control (-Leu -Trp) and selection (-Leu -Trp -Ade) plates and grown at 30 °C for 2–3 days before being scored for growth.

Results

The Meis protein UNC-62 plays multiple roles in the postembryonic M lineage

C. elegans contains two Meis-related genes, *unc-62* and *psa-3* (Van Auken et al., 2002 and Arata et al., 2006). We first examined the role of *psa-3* in the M lineage. Neither *psa-3(RNAi)* animals nor mutant animals homozygous for a loss-of-function *psa-3(os8)* allele (Arata et al., 2006) exhibited any M lineage defects, suggesting that *psa-3* is not likely to play a role in M lineage development. In contrast, animals with reduced levels of *unc-62* displayed multiple M lineage defects.

There are multiple *unc-62* alleles available, and the majority of them cause either zygotic or maternal-effect embryonic lethality (Van Auken et al., 2002). However, two weak zygotic alleles, *ku234* and *e644*, can produce viable progeny. *ku234* has a point mutation specifically affecting the start codon of the 1b isoforms, changing the first amino acid from Met to Ile, while *e644* has an early stop

Table 1
unc-62 genetically interacts with *ceh-20* and *mab-5* to regulate M lineage development.

Genotype[a]	*hlh-8*::*gfp* expression	Early M lineage phenotypes[b]	SM lineage phenotypes[c]
Wild-type	Bright (100%) *n* = 200	2 CCs, 2 SMs, 14 BWMs (100%) *n* = 200	4 VM1s (100%) *n* = 200
ceh-20(ay9)	Bright (80%) Faint[d] (20%) *n* = 200	2 CCs, 2 SMs, 14 BWMs (91%) 1–3 CCs, 1 SM and 13–14 BWMs (9%) *n* = 200[e]	4 VM1s (44%) >4 VM1s (56%) *n* = 75
unc-62(e644) dpy-11(e224)	Bright (100%) *n* = 200	2 CCs, 2 SMs, 14 BWMs (78%) 0–1 CCs, 3–4 SMs, 12–14 BWMs (22%) *n* = 200[f]	4 VM1s (44%) >4 VM1s (56%) *n* = 69
unc-62(ku234)	Bright (100%) *n* = 200	2 CCs, 2 SMs, 14 BWMs (100%) *n* = 200[g]	>4 VM1s (100%) *n* = 200
mab-5(RNAi)	No early expression Bright SM lineage expression (100%) *n* = 156	2 CCs, 2 SMs, 14 BWMs (6%) 0 CCs, 3–5 SMs, 13–14 BWMs (94%) *n* = 156	4 VM1s (6%) >4 VM1s (94%)
ceh-20(ay9)/+; unc-62(e644) dpy-11(e224)	Bright (100%) *n* = 123	2 CCs, 2 SMs, 14 BWMs (55%) 0–1 CCs, 3–4 SMs (45%) *n* = 60	4 VM1s (7%) >4 VM1s (93%) *n* = 123
ceh-20(ay9); unc-62(e644) dpy-11(e224)	Faint (3%) No expression (97%) *N* = 200	0–1 CCs[h] (100%) *n* = 83	>4 VM1s (100%) *n* = 45
ceh-20(ay9)/+; unc-62(ku234)/+	Bright (100%) *n* = 23	2 CCs, 2 SMs, 14 BWMs (100%) *n* = 23	4 VM1s (100%) *n* = 23
ceh-20(ay9)/+; unc-62(ku234)	Bright (100%) *n* = 163	2 CCs, 2 SMs, 14 BWMs (72%) 0–1 CCs, 2 SMs (28%) *n* = 163	>4 VM1s (100%) *n* = 163
ceh-20(ay9); unc-62(ku234)	Faint (7%) No expression (93%) *N* = 200	2 CCs, 2 SMs, 14 BWMs (13%) 0–1 CCs, 9–14 BWMs[i] (87%) *n* = 200	>4 VM1s (100%) *n* = 200
mab-5(RNAi); unc-62(e644) dpy-11(e224)	No expression (41%) Bright in SM lineage[j] (59%) *n* = 200	2 CCs (1%) 0–1 CCs[h] (99%) *n* = 200	0 VM1s[k] (58%) 4 VM1s (1%) >4 VM1s (41%) *n* = 200
mab-5(RNAi) ceh-20(ay9)	No expression (52%) Bright in SM lineage[j] (48%) *n* = 200	2 CCs (9%) 0–1 CCs[h] (91%) *n* = 200	0 VM1s[k] (60%) 4 VM1s (9%) >4 VM1s (31%) *n* = 200

[a] All animals examined carried the following GFP markers for the M lineage: *intrinsic CC*::*gfp(ccIs4438)* III, *ayIs2(egl-15*::*gfp)* IV; *hlh-8*::*gfp(ayIs6)* X.
[b] Phenotypes focus on specification of the 18 M lineage descendants (14 BWMs, 2 CCs and 2 SMs) produced at the L1 stage.
[c] The SM lineage phenotypes shown here focused on the number of *egl-15*::*gfp* expressing VM1-like cells.
[d] *hlh-8*::*gfp* signal was faint in both the early M lineage and the SM lineage.
[e] The number of BWMs was obtained via examining 6 animals.
[f] The number of BWMs was obtained via examining 5 animals.
[g] The number of BWMs was obtained via examining 3 animals.
[h] The number of BWMs and SMs was not determined in this mutant strain.
[i] The number of BWMs was obtained via examining 5 animals.
[j] There was no *hlh-8*::*gfp* expression in the early M lineage.
[k] Some of the animals had 1–3 elongated *egl-15*::*gfp* positive cells randomly located in the posterior of the worm.

codon in the homeodomain region encoded by exon 7b (Van Auken et al., 2002). We introduced the M lineage-specific GFP markers into *ku234* and *e644* mutants and examined their M lineage phenotypes.

The early M lineage appeared completely normal in *ku234* mutants, producing two SMs, two CCs and fourteen BWMs (Table 1, Fig. 1E). Just like in wild-type animals, the two SMs in *ku234* mutants migrated to the presumptive vulval region and underwent three rounds of division to produce 16 *hlh-8*::*gfp*-positive precursor cells. However, unlike wild-type animals in which the 16 sex muscle precursors differentiate into 8 vulval muscles (4 VM1s and 4 VM2s) and 8 uterine muscles (4 UM1s and 4 UM2s), in 100% ($n=200$) of *ku234* mutants examined, the majority (ranging between 9 and 14) of the 16 sex muscle precursor cells differentiated into VM1-like cells that expressed *egl-15*::*gfp* (Fig. 1E, compare Figs. 2A, B). These extra VM1-like cells appeared to be a result of fate transformation from UMs and VM2s to VM1s based on the following observations. First, in wild-type animals, *NdE-box*::*gfp* labels all 16 differentiated sex muscles while highlighting the distinct cell morphologies of VMs and UMs (Harfe et al., 1998; Fig. 2C). *ku234* mutants had 16 *Nde-box*::*gfp*-expressing cells; however, there was an increase of VM-like cells and a concomitant decrease of UM-like cells (Fig. 2D). Second, *rgs-2*::*gfp*, which preferentially labels UMs but also faintly labels VMs in wild-type animals (Kostas and Fire, 2002; Fig. 2E), showed an increase of the faint VM-like signal and a decrease of the bright UM-like signal in *ku234* mutants (Fig. 2F). Finally, all the eight vulval muscles (both VM1s and VM2s) in wild-type animals express *arg-1*::*gfp* (Kostas and Fire, 2002; Fig. 2G). *ku234* mutants had 10 to 14 *arg-1*::*gfp*-positive cells that all exhibited the morphology of VM1-like cells (Fig. 3H). Thus, most of the UMs and VM2s are transformed to VM1s in *ku234* mutants.

Previous work by Kostas and Fire (2002) showed that the T-box gene *mls-1* is a cell fate determinant of uterine muscles (UMs): *mls-1* is specifically expressed in the UM and VM2 precursor cells (Fig. 2I) and loss of *mls-1* activity results in the doubling of the numbers of both VM1s and VM2s due to a fate transformation of UMs to VMs. The *ku234* mutant phenotype is similar, but not identical, to that of *mls-1* mutants. We therefore tested if *mls-1* expression is affected in *unc-62(ku234)* mutants. We detected normal expression of a functional *mls-1*::*lacZ* reporter in the SM lineage of *ku234* mutants (Fig. 2J), suggesting that the UM to VM fate transformation in *ku234* mutants is not due to the loss of or altered *mls-1* expression.

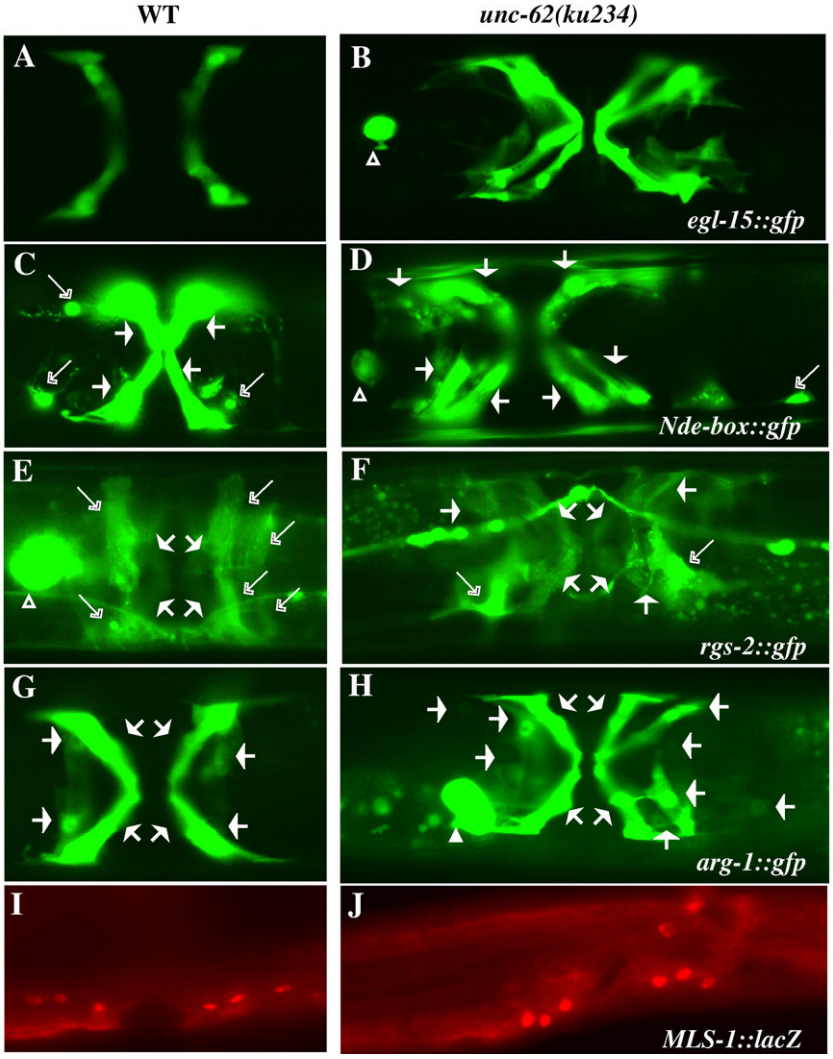

Fig. 2. Uterine muscles (UMs) and type II vulval muscles (VM2s) are transformed to type I vulval muscles (VM1s) in *unc-62(ku234)* mutants. Ventral views of wild-type (A, C, E, G) and *unc-62(ku234)* (B, D, F, H) animals showing the differentiated sex muscles. Four VM1s in wild-type (A) and 12 VM1s in *unc-62(ku234)* (B) animals visualized by *egl-15*::*gfp*. UMs and VMs visualized by *Nde-box*::*gfp* (C, D) and *rgs-2*::*gfp* (E, F) in wild-type (C, E) and *unc-62(ku234)* (D, F) animals. The morphology of UMs (marked by longer open arrows) and VMs (marked by short solid arrows) are distinct. *unc-62(ku234)* animals (D, F) have reduced numbers of cells with the UM morphology and extra numbers of cells with the VM morphology. *arg-1*::*gfp* in wild-type (G) and *unc-62(ku234)* (H) animals showing both VM1s and VM2s. The *unc-62(ku234)* animal in panel H has 12 VM1s. (I, J) *mls-1*::*lacZ* expression pattern in wild-type (I) and *unc-62(ku234)* (J) animals. Six out of the 12 (I) and 8 out of the 12 (J) *mls-1*::*lacZ*-expressing cells are shown in panels I and J, respectively. The other *mls-1*::*lacZ*-expressing cells are on a different focal plane. Both wild-type and *unc-62(ku234)* animals show similar *mls-1*::*lacZ* expression patterns.

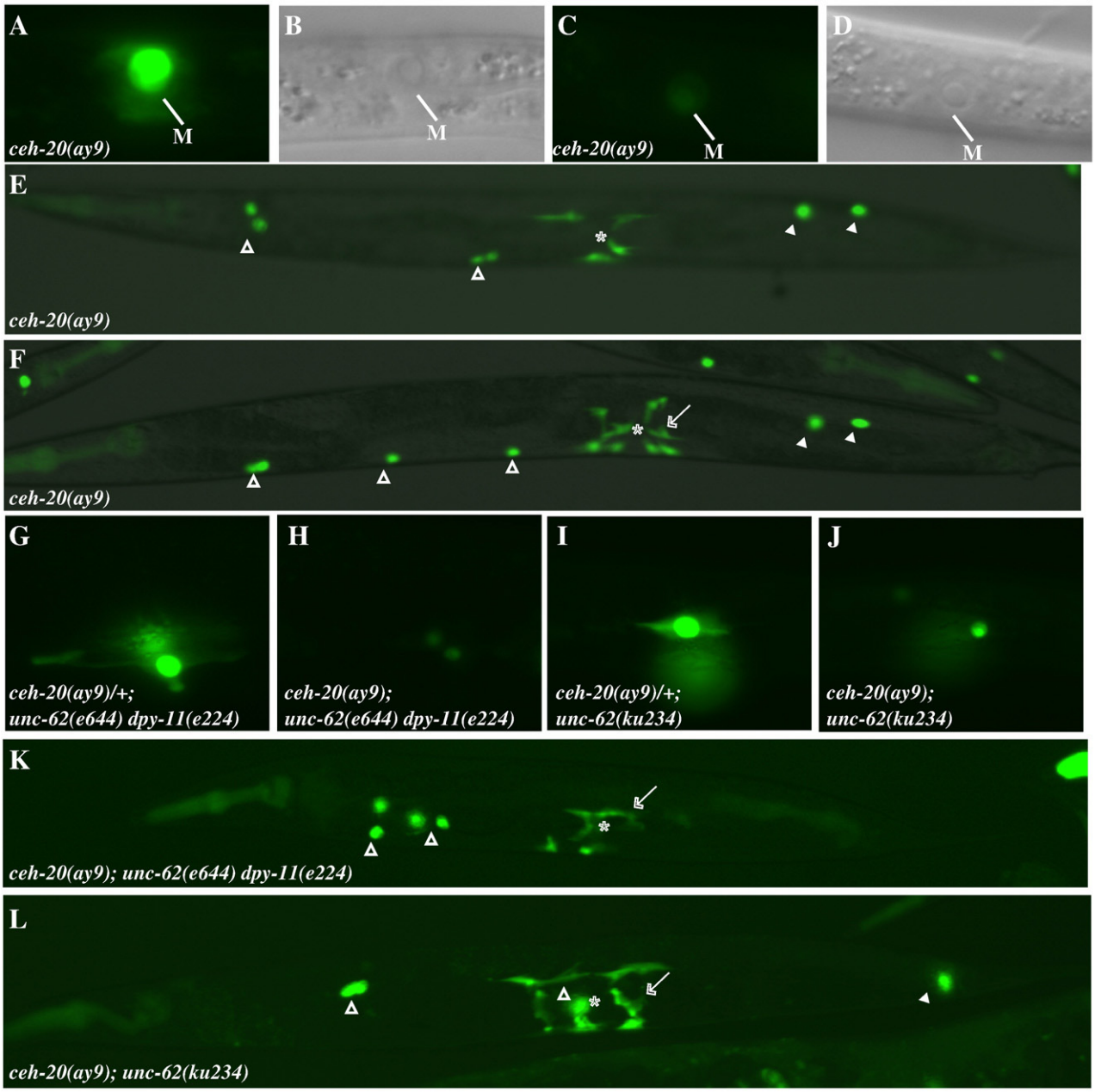

Fig. 3. *ceh-20* genetically interacts with *unc-62* to regulate M lineage development. (A–F) Various M lineage phenotypes of *ceh-20(ay9)* animals. (A–D) *ceh-20(ay9)* animals at the 1-M stage with *hlh-8*::*gfp* (A, C) and the corresponding DIC images (B, D). 80% ($n = 200$) of *ceh-20(ay9)* animals exhibit strong *hlh-8*::*gfp* expression (A), while 20% showing much reduced *hlh-8*::*gfp* expression (C). Panels A and C are under the same exposure. (E, F) Adult *ceh-20(ay9)* animals visualized using an *intrinsic CC*::*gfp* and *egl-15*::*gfp*. (E) An *ay9* animal with the normal number of M-derived CCs and VM1s that are not properly attached. (F) An *ay9* animal with the normal number of M-derived CCs but a total number of 10 VM1s. (G–J) *hlh-8*::*gfp* expression in the 2 SMs of *ceh-20(ay9)/+; unc-62(e644) dpy-11(e224)* (G), *ceh-20(ay9); unc-62(e644) dpy-11(e224)* (H), *ceh-20(ay9)/+; unc-62(ku234)* (I) and *ceh-20(ay9); unc-62(ku234)* (J) animals. Notice the reduced level of *hlh-8*::*gfp* expression in *ceh-20(ay9); unc-62(e644) dpy-11(e224)* (H) and *ceh-20(ay9); unc-62(ku234)* (J) animals compared to that in *ceh-20(ay9)/+; unc-62(e644) dpy-11(e224)* (G) and *ceh-20(ay9)/+; unc-62(ku234)* (I) animals. (K, L) Adult *ceh-20(ay9); unc-62(e644) dpy-11(e224)* (K) and *ceh-20(ay9); unc-62(ku234)* (L) animals visualized using an *intrinsic CC*::*gfp* and *egl-15*::*gfp*. (K) A *ceh-20(ay9); unc-62(e644) dpy-11(e224)* animal with no M-derived CCs and extra VM1s. (L) A *ceh-20(ay9); unc-62(ku234)* animal with one M-derived CCs and extra VM1s. Open arrowheads: embryonically-derived CCs. Solid arrowheads: M-derived CCs. Arrows: ectopic *egl-15*::*gfp*-expressing VM1-like cells. *: Location of the vulva.

Unlike *ku234* mutants, *e644* mutants exhibited variable M lineage defects. We used *hlh-8*::*gfp* to follow the M lineage in *e644* mutants as *hlh-8*::*gfp* expression appeared unaffected in *e644* mutants. Among 200 *e644* worms examined, 22% of them had fewer (0–1) M-derived CCs and extra (3–4) SMs (Table 1). Direct observation of M lineage cell divisions in three *e644* animals showed that while M lineage patterning and proliferation were normal, both M-derived CCs and 1 or 2 M-derived BWMs were transformed to SMs (data not shown). The remaining 78% of *e644* animals contained normal numbers of SMs; however, 69% of these mutant animals with 2 SMs ($n = 69$) gave rise to extra VM1s, ranging from 5 to 10 (Fig. 1D, Table 1). Using the cell type specific GFP markers that were used for analyzing the *ku234* mutants, we found that these extra VM1s were produced at the expense of UMs and VM2s (data not shown), similar to the phenotypes observed in the *ku234* mutants. The multiple M lineage defects in *e644* mutants suggest that *unc-62* is not only involved in UM and VM decisions in the SM lineage, but also involved in CC, SM and BWM cell fate decisions in the early M lineage.

Because both *ku234* and *e644* are partial loss-of-function alleles of *unc-62* and *unc-62* is essential for embryogenesis (Van Auken et al.,

2002), we also soaked synchronized L1 wild-type worms with dsRNA against *unc-62* (referred to as *unc-62(RNAi-soaking)*, see Materials and methods) and examined the M lineage phenotypes in the soaked animals. Soaking buffer alone was used as a negative control. Unlike the control animals, *unc-62(RNAi-soaking)* worms exhibited defects in the vulva and the somatic gonad (data not shown), as well as in the M lineage. The M lineage phenotypes can be grouped into two categories. The majority of *unc-62(RNAi-soaking)* worms (87%, $n=137$) had no differentiated M-derived CCs, VM1s, or BWMs (Fig. 1F), or occasionally no M-derived CCs and BWMs, but with 1–4 elongated *egl-15::gfp*-positive cells (data not shown). These phenotypes resemble phenotypes observed in *ceh-20(RNAi)* or *lin-39(0) mab-5(0)* mutants (Liu and Fire, 2000). Unlike *ceh-20(RNAi)* or *lin-39 (0) mab-5(0)* mutants in which *hlh-8::gfp* expression is undetectable throughout postembryonic development (Liu and Fire, 2000), *unc-62 (RNAi-soaking)* worms showed normal *hlh-8::gfp* expression in the early M lineage during the L1 stage when CC, SM and BWM fates are specified. The early expression of *hlh-8::gfp* in the *unc-62(RNAi-soaking)* worms is likely due to the timing of soaking being too late to affect the early M lineage. The remaining 13% of *unc-62(RNAi-soaking)* animals had *hlh-8::gfp* expression throughout the M lineage, but exhibited fate transformation from one or both M-derived CCs to SMs (Fig. 1G) and randomized division orientation in the SM lineage (data not shown).

The range of M lineage defects observed in *unc-62(RNAi-soaking)* animals and in *ku234* and *e644* mutants suggest that *unc-62* plays multiple roles at multiple stages in the M lineage, including regulating CC/SM/BWM fate specification and differentiation, and VM/UM fate specification.

Analysis of a weak ceh-20 allele, ay9, revealed multiple roles of the PBC protein CEH-20 in the M lineage

We have previously shown that CEH-20, but not CEH-40, is the PBC protein that functions in the M lineage (Liu and Fire, 2000; Jiang et al., 2008). Furthermore, CEH-20 is required for the diversification of the M lineage (Liu and Fire, 2000). These previous studies are based on analyses of *ceh-20(RNAi)* and a strong loss-of-function allele *n2513*. We extended our analysis to additional alleles of *ceh-20*, including *os114* and *os39* (Arata et al., 2006), and *ay42* and *ay9* (Takacs-Vellai et al., 2007). Among these alleles, *os114* and *os39* appear to be the strongest loss-of-function, and possibly null, alleles of *ceh-20*, as 99% of *os114* and *os39* mutant animals ($n=87$ for *os114* and $n=56$ for *os39*) failed to generate any M lineage descendants, consistent with previous studies of *ceh-20(RNAi or n2513)* (Liu and Fire, 2000). *ay42* is likely a partial loss-of-function allele as 62% of *ay42* worms ($n=224$) failed to produce any M lineage products (data not shown).

ay9 contains a missense mutation, changing a highly conserved Met78 residue to Ile (Takacs-Vellai et al., 2007), and exhibits multiple M lineage phenotypes. In *ay9* mutant animals, *hlh-8::gfp* expression was detectable throughout the M lineage; however, compared to wild-type worms, the intensity of *hlh-8::gfp* signal was moderately decreased throughout the M lineage in 20% of *ay9* mutants ($n=200$) (Figs. 3A–D). All *ay9* mutants exhibited normal M lineage patterning and proliferation; however, 9% of *ay9* animals examined ($n=200$) exhibited earlier defects in CC/SM/BWM fate decisions, resulting in variable numbers of M-derived CCs, SMs, and BWMs in *ay9* mutants (Table 1). In addition to these earlier M lineage defects, *ay9* mutants also exhibited defects in the SM lineage. 56% of the *ay9* animals ($n=75$) that contained the normal number of SMs exhibited fate transformations from UMs and VM2s to VM1s, resulting in an increase of the number of *egl-15::gfp*-positive VM1s (5–10 VM1s) in *ay9* mutants (Table 1, Fig. 3F). VM1s often did not display proper orientation and attachment (Fig. 3E), likely due to the vulval defects in *ay9* mutants.

The broad range of M lineage defects seen in the various *ceh-20* mutant animals suggest that like *unc-62*, *ceh-20* plays multiple roles at multiple stages in the M lineage, including regulating CC/SM/BWM fate specification, VM/UM fate specification and *hlh-8* expression.

unc-62 genetically interacts with ceh-20 and mab-5 to regulate hlh-8/CeTwist expression and cell fate specification in the M lineage

The similar M lineage defects caused by mutations or RNAi of *unc-62* and *ceh-20* suggest that *unc-62* and *ceh-20* may function together to regulate proper M lineage development. To test this hypothesis, we generated double mutants between *ceh-20(ay9)* and *unc-62(e644)* or *unc-62(ku234)*.

Compared to *unc-62(e644)* single mutants, *ceh-20*(*ay9*)/+; *unc-62* (*e644*)/*unc-62*(*e644*) animals showed a roughly 20% increase (from 22% to 45%) in penetrance of fate transformations from M-derived CCs to SMs (Table 1). *ceh-20(ay9); unc-62(e644)* double homozygous animals exhibited significantly more penetrant and severe M lineage defects compared to *ceh-20(ay9)* and *unc-62(e644)* single mutants (Table 1). First, unlike in each single mutant, *hlh-8::gfp* was undetectable (97%) or very faint (3%, $n=200$) throughout the M lineage in *ceh-20(ay9); unc-62(e644)* double mutants (Figs. 3G, H). Second, 100% of *ceh-20(ay9); unc-62(e644)* double mutants ($n=83$) had no M-derived CCs, compared to 9% ($n=200$) of *ceh-20(ay9)* animals and 22% ($n=200$) of *unc-62(e644)* animals that had a CC to SM fate transformation (Table 1, Fig. 3K). Thus there appeared to be a dose-dependent effect of *ceh-20* on *unc-62*(*e644*) mutants regarding *hlh-8* expression and early M lineage fate specification. Similar synergistic effect on M lineage development was also observed between *ceh-20*(*ay9*) and *unc-62*(*ku234*) (Table 1, Figs. 3I, J, L). These observations are consistent with *ceh-20* and *unc-62* functioning together in regulating fate specification and *hlh-8::gfp* expression during M lineage development. In addition to the M lineage defects, we also observed enhanced penetrance of embryonic lethality and vulval defects in *ceh-20; unc-62* double mutants (data not shown), suggesting that these two genes function together in multiple tissues at multiple developmental stages.

In addition to the genetic interactions between *unc-62* and *ceh-20*, we also observed genetic interactions between *unc-62* and the Hox gene *mab-5*. *mab-5(0)* or *mab-5(RNAi)* mutants lack *hlh-8::gfp* expression in the early M lineage, but show normal *hlh-8::gfp* expression in the SM lineage. Furthermore, the M-derived CCs and 1–3 M-derived BWMs are transformed to SMs in *mab-5(0)* or *mab-5(RNAi)* mutants (Harfe et al., 1998; Liu and Fire, 2000; Amin et al., 2007, Table 1). 41% ($n=85$) of *mab-5(RNAi); unc-62(e644)* mutant animals showed no *hlh-8::gfp* expression throughout the M lineage, lacked all M-derived CCs, and had zero or 1–5 elongated *egl-15::gfp* positive cells. These phenotypes resemble those observed in *lin-39(0) mab-5(0)* and *ceh-20 (RNAi)* animals (Liu and Fire, 2000). These observations suggest that in addition to *ceh-20*, *unc-62* also functions together with the Hox gene *mab-5* to regulate *hlh-8::gfp* expression and M lineage fate specification. Similar synergistic interactions were also observed in *mab-5 (RNAi) ceh-20(ay9)* animals (Table 1), consistent with previous findings on the cooperative actions of *mab-5* and *ceh-20* in regulating *hlh-8* expression and M lineage fate specification.

unc-62 and ceh-20 are co-expressed throughout the M lineage and in other cell types

Because *ceh-20* and *unc-62* appear to function together to regulate multiple processes of M lineage development at multiple developmental stages, we next determined when and where these two genes are expressed in the M lineage.

unc-62 uses two alternative start codons, exon 1a or 1b (Van Auken et al., 2002). To determine the temporal and spatial expression pattern of *unc-62*, we generated a transcriptional *gfp* reporter (*unc-62p::gfp*) using 2.9 kb sequences upstream of the start codon of exon 1a (see Materials and methods). We first found that *unc-62* cDNAs under the control of this 2.9 kb promoter element can rescue the M

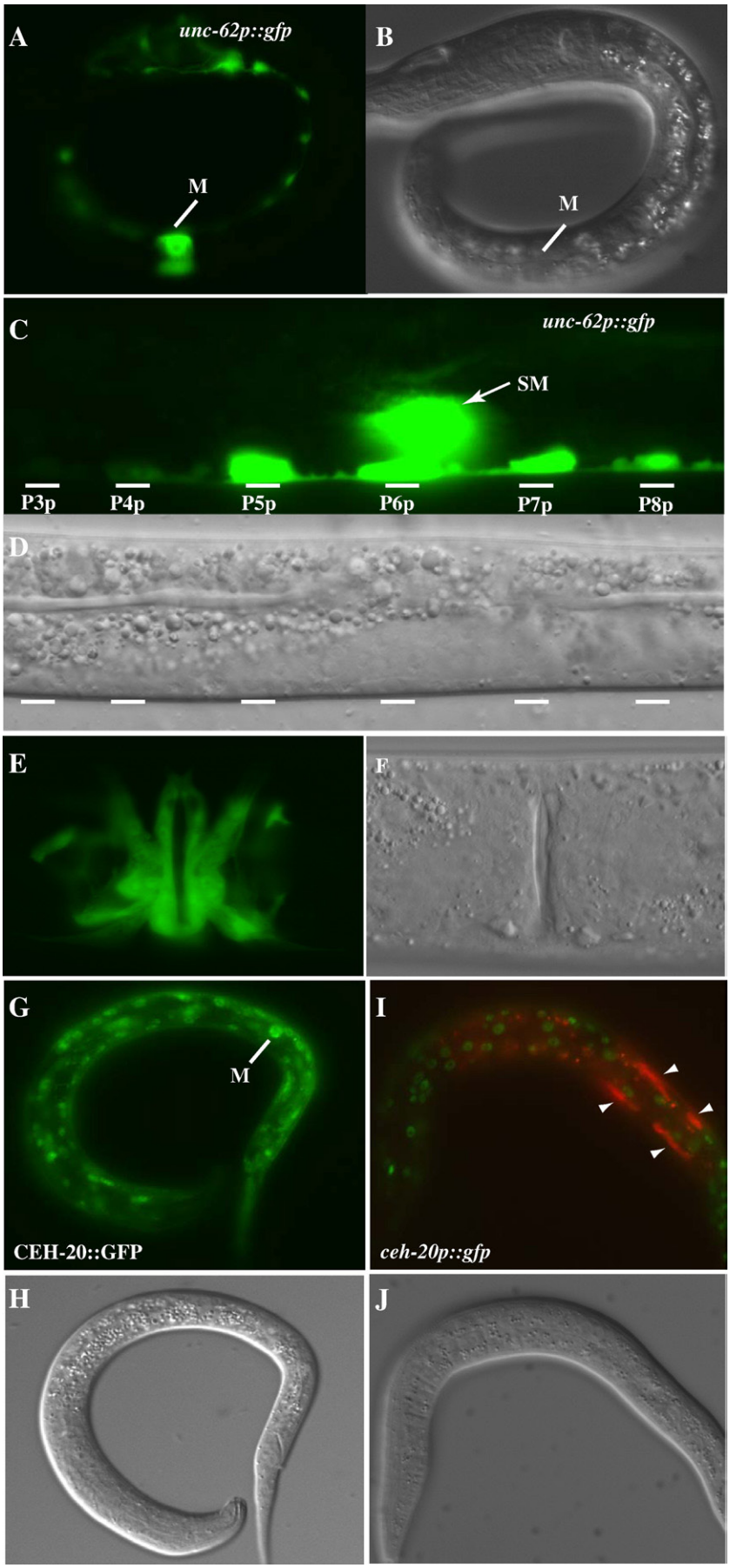
A
unc-62p::gfp
M
B
M
C
unc-62p::gfp
SM
P3p
P4p
P5p
P6p
P7p
P8p
D
E
F
G
M
CEH-20::GFP
I
ceh-20p::gfp
H
J

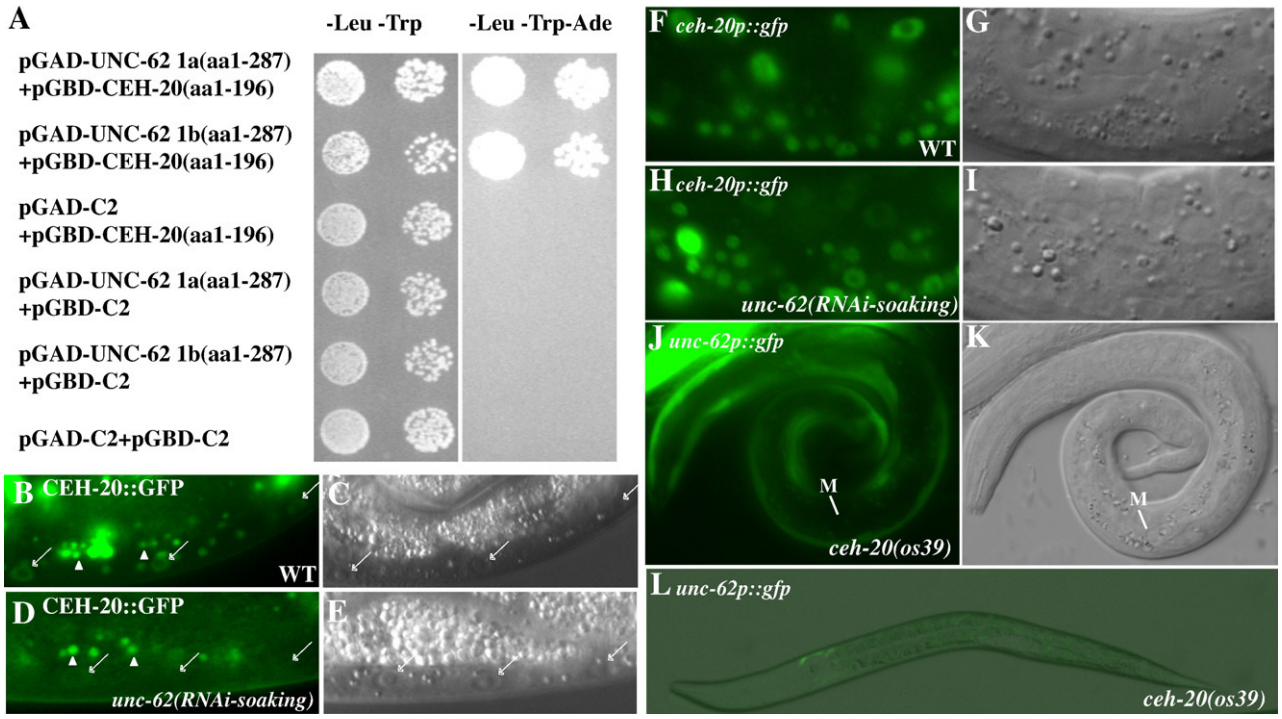

Fig. 5. UNC-62 and CEH-20 exhibit physical and regulatory interactions. (A) The N-termini of both the 1a and 1b splicing isoforms of *unc-62* that contain the HM domain can bind to the PBC domain (aa 1–196) of CEH-20 in the yeast two-hybrid assay. Interaction was detected in one direction using the PBC domain (aa 1–196) of CEH-20 fused to the GAL4 DNA-binding domain (GBD). The GBD-UNC-62 fusions autoactivate and were not included in the tests. (B–E) CEH-20::GFP (B, D) and the corresponding DIC images (C, E) in wild-type (B, C) and *unc-62(RNAi-soaking)* (D, E) animals. CEH-20::GFP is present in the nucleus, but not the nucleolus, of multiple cell types in wild-type animals (B, C). Notice the significant reduction or loss of nuclear CEH-20::GFP in *unc-62(RNAi-soaking)* animals (arrows in panel D) compared to wild-type animals (arrows in panel B). Additional bright gut autofluorescence signals in panels B and D are marked by arrowheads. (F–I) *ceh-20p::gfp* (F, H) and the corresponding DIC images (G, I) in wild-type (F, G) and *unc-62(RNAi-soaking)* (H, I) animals. The expression of the transcriptional *ceh-20p::nls::gfp* is not affected by *unc-62(RNAi-soaking)*. (J–L) *unc-62p::gfp* in *ceh-20(os39)* animals. Expression of *unc-62p::gfp* is lost in the M cell in an L1 animal (J–K) and most of the cells in an L2 animal (L).

lineage defects of *unc-62(e644)* and *unc-62(ku234)* mutants. We then examined the expression pattern of *unc-62p::gfp* in transgenic animals carrying the reporter construct. Similar GFP expression patterns were observed in three independent transgenic lines. *unc-62p::gfp* expression was first detectable during mid-embryogenesis in a subset of cells that include AB lineage derivatives (data not shown). In newly hatched L1 larvae, *unc-62p::gfp* was observed in multiple cell types including the M mesoblast, as well as a few neurons in the head and tail, and dorsal and ventral hypodermis (Figs. 4A, B). In the L1 larva, *unc-62p::gfp* expression continued throughout the M lineage in all dividing M descendants (data not shown). The GFP signal was transiently detectable in M-derived CCs and BWMs before they terminally differentiate, but remained detectable in the SMs (Figs. 4C, D) and throughout the SM lineage (data not shown), including the differentiated vulval muscles (Figs. 4E, F). Outside of the M lineage, the neuronal expression in the head and tail was retained throughout postembryonic development, while hypodermal expression appeared more variable. *unc-62p::gfp* expression was also observed in a subset of ventral nerve cord (VNC) cells after the L2 stage (data not shown) and in the P lineage with initial faint GFP expression in P3.p, P4.p and P5.p in L1 animals, which expanded to P6.p, P7.p and P8.p cells at the L2 stage (Figs. 4C, D). Upon vulval induction, L3 and L4 larvae displayed strong GFP expression in P5.p, P6.p and P7.p and their descendants, but expression in P3.p, P4.p and P8.p and their descendants became weaker and eventually undetectable by mid-L4 stage. *unc-62p::gfp* expression persisted in all differentiated vulval cells after vulval morphogenesis in adults (data not shown).

ceh-20 shared an overlapping, but not identical, expression pattern with *unc-62* both within and outside of the M lineage. Using a functional *ceh-20::gfp* construct (see Materials and methods), we detected nuclear GFP signal in a wide array of cells outside of the M lineage, including a subset of embryonic cells, hypodermal cells, gut cells, bodywall muscles, VNC neurons and VPCs (data not shown), consistent with previous reports on the expression pattern of *ceh-20* (Yang et al., 2005; Liu et al., 2006; Takacs-Vellai et al., 2006). Within the M lineage, CEH-20::GFP was detected in the M cell (Figs. 4G, H) and throughout the early M lineage. It persisted in the differentiated BWMs as well as in the SMs and all the SM descendants (data not shown). In addition to the translational *gfp* reporter, we also generated a transcriptional *ceh-20p::gfp* reporter (see Materials and methods). Transgenic animals carrying *ceh-20p::gfp* showed a similar expression pattern to the translational *ceh-20::gfp* reporter outside of the M lineage, but failed to show expression in the M lineage (Figs. 4I, J). Because the only difference between the translational *ceh-20::gfp* and the transcriptional *ceh-20p::gfp* constructs is the presence or absence of the introns, the above observations suggest that the introns of *ceh-20* may contain enhancer elements(s) required for *ceh-20* expression in the M lineage.

Fig. 4. Both *unc-62* and *ceh-20* are expressed in the M lineage. (A–F) *unc-62p::gfp* (A, C, E) and corresponding DIC images (B, D, F) of 1-M stage L1 (A, B), 2-SM stage L2 (C, D) and adult stage animals. *unc-62p::gfp* is expressed throughout the M lineage, including mature vulval muscles (E) and in the P lineages (C). (G–J) GFP (G, I) and corresponding DIC images showing the expression of a functional translational CEH-20::GFP in the M mesoblast (G, H) and the lack of M lineage expression of the transcriptional *ceh-20p::gfp* in the M lineage (I, J). Green in I: *ceh-20p::gfp*. Red in I: *hlh-8p::rfp*. Notice that *ceh-20p::gfp* is expressed in the other cell types that express CEH-20::GFP, but not in cells of the M lineage (marked by arrowheads).

The similar expression patterns of *unc-62* and *ceh-20* throughout the M lineage are consistent with their multiple and cooperative roles in the M lineage, as indicated by the genetic interactions described earlier.

unc-62 and ceh-20 display physical and regulatory interactions

Because both *unc-62* and *ceh-20* share similar expression patterns in the M lineage, the synergistic interactions between them could be due to direct physical interactions between these two factors, or regulatory interactions, or both. To test these possibilities, we first used the yeast two-hybrid system and tested whether UNC-62 and CEH-20 can interact with each other. When fused with the GAL4 DNA-binding domain, full length UNC-62 and CEH-20 each alone activated reporter expression (data not shown). We thus made truncations of each protein and found that the region containing the PBC domain of CEH-20 (aa1–196) interacts with the N-terminal 287aa (isoform 1a) or 250aa (isoform 1b) of UNC-62, which contains the HM domain (Fig. 5A). These results suggest that CEH-20 and UNC-62 can physically interact with each other.

Previous studies have shown that *unc-62* is required for the nuclear localization of CEH-20 (Van Auken et al., 2002; Potts et al., 2009). Consistent with these findings, we found that *unc-62(RNAi)* led to the reduction of the translational CEH-20::GFP signal (Figs. 5B–E), but not the transcriptional *ceh-20p::gfp* signal (Figs. 5F–I). To determine whether CEH-20 plays a role in regulating the expression of *unc-62*, we assayed the expression of the *unc-62p::gfp::let-858* 3′ UTR reporter in the strong loss-of-function, and possibly null, alleles of *ceh-20*, *os39*. We found that 96 of 97 *ceh-20(os39)* mutant animals lacked *unc-62p::gfp* signal in the M mesoblast and the P lineages, but did express *unc-62p::gfp* in neuronal or hypodermal cells (Figs. 5J–L). Similar observations were made using the strong loss-of-function *ceh-20(n2513)* mutants (data not shown). Since the M mesoblast is still present in the *os39* mutant animals and the *unc-62p::gfp* reporter uses the well characterized *let-858* 3′ UTR (Kelly et al., 1997), the above results suggest that *ceh-20* is required to positively regulate the promoter activity of *unc-62* in the M lineage and P lineage, but not in neuronal or hypodermal cells.

Discussion

Meis/hth/unc-62 functions in mesodermal development

MEIS family proteins have been previously shown to play important roles in multiple aspects of development in both vertebrates and invertebrates (for example, see Abu-Shaar and Mann, 1999; Henderson and Andrew, 2000; Choe et al., 2002; Choe and Sagerstrom, 2004; Mercader et al., 2005). Similarly, the *C. elegans* MEIS-related proteins *psa-3* and *unc-62* have been shown to function in regulating T cell asymmetric cell division (*psa-3*, Arata et al., 2006), regulate embryogenesis, Q neuroblast migration, vulval formation and VC motor neuron survival (*unc-62*, Van Auken et al., 2002; Yang et al., 2005; Potts et al., 2009). In this study, we have found that a loss-of-function mutation *psa-3(os8)* or *psa-3(RNAi)* did not affect the postembryonic mesodermal lineage, the M lineage. However, reducing *unc-62* activity led to pleiotropic M lineage phenotypes including defects in cell fate specification and differentiation, indicating that *unc-62* is a crucial regulator of mesodermal development in *C. elegans*.

In *Drosophila*, the MEIS protein Hth functions in the visceral mesoderm to regulate *dpp* expression (Stultz et al., 2006). Murine *meis-2* exhibits a dynamic expression pattern in differentiating somitic mesodermal cells (Cecconi et al., 1997). Similar temporal expression of *meis-2* has also been observed in the lateral mesoderm in zebrafish (Biemar et al., 2001; Zerucha and Prince, 2001). Thus MEIS family proteins may share a conserved role in mesodermal development.

UNC-62 functionally cooperates with CEH-20 to regulate mesoderm development

Previous work has shown that *ceh-20* is required for the specification and diversification of the M lineage, as well as the proper specification of CC and BWM fates (Liu and Fire, 2000). Our analysis of the phenotypes of a weak *ceh-20(ay9)* allele revealed another role of *ceh-20* in the proper specification of uterine muscles (UMs) and vulval muscles (VMs). *ceh-20* and *unc-62* appear to function together in this process, as two partial loss-of-function *unc-62* alleles, *e644* and *ku234*, both caused fate transformations from UMs and type II vulval muscles (VM2s) to type I vulval muscles (VM1s). In particular, the *ku234* mutants exhibited 100% penetrance of the UM and VM2 to VM1 fate transformation without affecting the early M lineage (Table 1, Fig. 2). Because *ku234* is a point mutation located in the first intron of the 1a isoform, but mutating the translation initiation codon of the 1b isoform, either the *ku234* mutation disrupts a VM/UM precursor-specific enhancer element located in the first intron, or the 1b isoform of *unc-62* is specifically expressed in the VM/UM precursor cells. *unc-62* is also required for proper specification and differentiation of M-derived CCs and BWMs. In addition to the similar M lineage phenotypes shared by *ceh-20* and *unc-62* mutants, we observed synergistic genetic interactions between *ceh-20* and *unc-62*. As shown in Table 1, both *ceh-20(ay9); unc-62(e644)* and *ceh-20(ay9); unc-62(ku234)* double mutants exhibited more severe M lineage defects compared to each of the corresponding single mutants. For example, even though *unc-62 (ku234)* single mutants did not exhibit any early M lineage defects, the *ceh-20(ay9); unc-62(ku234)* double mutant animals showed severe early M lineage defects in CC/BWM/SM fate specification.

The genetic interactions between *unc-62* and *ceh-20* could be due to 1) a physical interaction, 2) regulatory interactions, or 3) both physical and regulatory interactions between the two factors. We have found that *unc-62* and *ceh-20* share similar expression patterns within and outside of the M lineage, and that they can physically interact in the yeast two-hybrid system. We further showed that the two genes also share regulatory interactions: while *unc-62* is required for the nuclear localization of the CEH-20 protein, *ceh-20* is required for the expression of *unc-62* in the M lineage. Because the M cell is present in *ceh-20* mutants and the *unc-62p::gfp* reporter uses the well characterized *let-858* 3′ UTR (Kelly et al., 1997), the lack of expression of the *unc-62p::gfp* reporter in the M and P lineages in *ceh-20* mutants suggests that *ceh-20* may positively regulate the transcription of *unc-62*. However, at this point, we do not know whether this regulation is direct or indirect. The regulation of the nuclear localization of PBC proteins by MEIS proteins have been previously reported in multiple systems (Pai et al., 1998; Abu-Shaar et al., 1999; Affolter et al., 1999; Berthelsen et al., 1999; Jaw et al., 2000; Rieckhof et al., 1997; Potts et al., 2009). However, transcriptional regulation of MEIS by PBC proteins has not been previously reported. In *Drosophila*, *hth* transcription appears not to be affected by the loss of *exd* (Abu-Shaar and Mann, 1998) even though Hth protein level is greatly reduced in embryos lacking both maternal and zygotic EXD (Kurant et al., 1998) or in *exd* mutant clones (Abu-Shaar and Mann, 1998). Thus our findings add one more level to the complex interactions between MEIS and PBC family of proteins: possible transcriptional regulation of *meis* genes by PBC proteins.

The MEIS and PBC proteins have been implicated as cofactors of Hox proteins that cooperatively bind to target DNA sequences with Hox proteins (Maconochie et al., 1997; Kroon et al., 1998; Swift et al., 1998; Ryoo et al., 1999; Shanmugam et al., 1999; Shen et al., 1999; Ferretti et al., 2000; Ebner et al., 2005). The early M lineage defects of *unc-62(e664)*, *unc-62(RNAi-soaking)* and *ceh-20(ay9)* mutants regarding CC/BWM/SM fate specification and differentiation are very similar to the previously described phenotypes of *mab-5(0)* mutants (Harfe et al., 1998). Furthermore, the *ceh-20(ay9); unc-62(e644),*

ceh-20(ay9); unc-62(ku234), *mab-5(RNAi); unc-62(e644)* and *mab-5 (RNAi) ceh-20(ay9)* double mutants exhibited more severe M lineage phenotypes that resemble the *lin-39(0) mab-5(0)* double mutant phenotypes. These observations suggest that UNC-62 may interact with CEH-20 and Hox to activate downstream targets required for the diversification and proper BWM/CC/SM fate specification of the M lineage. At this point, it is not clear whether the cooperative role of UNC-62 and CEH-20 in UM/VM fate specification is dependent on the Hox factors. *lin-39(0)* mutants have no defects in the M lineage, while *lin-39(0) mab-5(0)* mutants and *mab-5(0)* mutants both have earlier defects in the M lineage, which could potentially mask the role of *mab-5* and *lin-39* in the late SM lineage.

It has been shown that LIN-39 or MAB-5 and CEH-20 can form heterodimers and bind to the corresponding Hox-PBC binding sites in the promoter region of *hlh-8* to regulate its expression (Liu and Fire, 2000). Since *hlh-8::gfp* expression is absent or barely detectable in *ceh-20(ay9); unc-62(e644)*, *ceh-20(ay9); unc-62(ku234)*, *mab-5 (RNAi); unc-62(e644)* and *mab-5(RNAi) ceh-20(ay9)* mutants, it is possible that UNC-62 may participate in the DNA-bound Hox–CEH-20 complex in regulating *hlh-8* expression. However, we did not find any potential MEIS binding site (TGACAG, Chang et al., 1997; Knoepfler et al., 1997; Shen et al., 1999; Berthelsen et al., 1999) adjacent to the Hox–CEH-20 consensus sequence in the characterized *hlh-8* promoter region (Liu and Fire, 2000). Furthermore, attempts using chromatin immunoprecipitation (ChIP) on the *hlh-8* promoter failed, possibly due to the short time window of early M lineage development and the small number of M-derived cells (1–18) relative to the whole animal (~900 somatic cells). It is possible that UNC-62 binds to some novel sequences in the *hlh-8* promoter that are different from the canonical MEIS binding site, or UNC-62 acts as a non-DNA-binding partner in the Hox-CEH-20-UNC-62 trimeric complex. The physical interaction that we observed between CEH-20 and UNC-62 is consistent with the second hypothesis.

In addition to regulating *hlh-8* expression, *unc-62* and *ceh-20* may have additional targets in the M lineage. We have previously found that the HMX factor MLS-2 is likely a direct target of CEH-20 in the M lineage (Jiang et al., 2008). We observed normal *mls-2* expression in the early M lineage of *unc-62(RNAi-soaking)* animals (data not shown). However, since *unc-62(RNAi-soaking)* may not completely knock out *unc-62* activity in the early M lineage, we cannot rule out the possibility that *mls-2* is regulated by *unc-62*.

In the SM lineage, a T-box transcription factor MLS-1 is both necessary and sufficient for UM fate specification (Kostas and Fire, 2002). *mls-1* is expressed in both UM and VM2 precursor cells and is regulated by *hlh-8* (Kostas and Fire, 2002). While *unc-62(ku234)* mutants exhibited fate transformations from UMs and VM2s to VM1s (Figs. 2A–H), *mls-1* expression appeared normal (Figs. 2I, J). Thus, *unc-62* must be involved in regulating *mls-1* activity through post-transcriptional processes. For instance, *unc-62* could be required to activate MLS-1 cofactor(s) in the SM lineage, which then function(s) together with MLS-1 to promote UM fate.

In summary, UNC-62/MEIS/HTH, CEH-20/PBX/EXD and Hox factors (MAB-5 and LIN-39) play multiple roles in the *C. elegans* postembryonic mesoderm. Previous work have found roles of CEH-20 and Hox factors MAB-5 and LIN-39 in cell proliferation in the M lineage as well as in the specification and differentiation of M lineage-derived striated bodywall muscles (BWMs) and non-muscle coelomocytes (CCs) (Harfe et al., 1998; Liu and Fire, 2000; Jiang et al. (2008). We showed in this work that UNC-62 also participates in these functions. Furthermore, we demonstrated that UNC-62 and CEH-20 are also required for the proper specification of non-striated vulval and uterine muscles (VM and UMs). While all three factors are required for the M lineage expression of CeTwist, HLH-8 (Liu and Fire, 2000; this work), CEH-20 appears to function in a Hox-independent manner in regulating the HMX gene *mls-2* (Jiang et al., 2005, 2008). The mode in which these three factors function together or independently will be elucidated upon the identification and characterization of additional M lineage-specific targets of each.

Acknowledgments

We thank the *C. elegans* Genetics Center (which is funded by the NIH), Thomas Bürglin, Yuji Kohara, Hitoshi Sawa, Lois Edgar and Bill Wood for strains and plasmids; Nirav Amin and Chenxi Tian for helpful discussions and valuable comments on the manuscript. This work was supported by NIH R01 GM066953 (to J.L.).

References

Abu-Shaar, M., Ryoo, H.D., Mann, R.S., 1999. Control of the nuclear localization of extradenticle by competing nuclear import and export signals. Genes Dev. 13, 935–945.
Affolter, M., Marty, T., Vigano, M.A., 1999. Balancing import and export in development. Genes Dev. 13, 913–915.
Ahringer, J., 2006. Reverse genetics. In: The *C. elegans* Research Community, editor. Wormbook. http://www.wormbook.org.
Amin, N.M., Hu, K., Pruyne, D., Terzic, D., Bretscher, A., Liu, J., 2007. A Zn-finger/FH2-domain containing protein, FOZI-1, acts redundantly with CeMyoD to specify striated body wall muscle fates in the *Caenorhabditis elegans* postembryonic mesoderm. Development 134, 19–29.
Arata, Y., Kouike, H., Zhang, Y., Herman, M.A., Okano, H., Sawa, H., 2006. Wnt signaling and a hox protein cooperatively regulate Psa-3/Meis to determine daughter cell fate after asymmetric cell division in *C. elegans*. Dev. Cell 11, 105–115.
Berthelsen, J., Kilstrup-Nielsen, C., Blasi, F., Mavilio, F., Zappavigna, V., 1999. The subcellular localization of PBX1 and EXD proteins depends on nuclear import and export signals and is modulated by association with PREP1 and HTH. Genes Dev. 13, 946–953.
Biemar, F., Devos, N., Martial, J.A., Driever, W., Peers, B., 2001. Cloning and expression of the TALE superclass homeobox meis2 gene during zebrafish embryonic development. Mech. Dev. 109, 427–431.
Brenner, S., 1974. The genetics of Caenorhabditis elegans. Genetics 77, 71–94.
Burglin, T.R., 1997. Analysis of TALE superclass homeobox genes (MEIS, PBC, KNOX, Iroquois, TGIF) reveals a novel domain conserved between plants and animals. Nucleic Acids Res. 25, 4173–4180.
Burglin, T.R., 1998. The PBC domain contains a MEINOX domain: coevolution of Hox and TALE homeobox genes? Dev. Genes Evol. 208, 113–116.
Bürglin, T.R., Ruvkun, G., 1992. New motif in PBX genes. Nature Genet. 1, 319–320.
Cecconi, F., Proetzel, G., Alvarez-Bolado, G., Jay, D., Gruss, P., 1997. Expression of Meis2, a knotted-related murine homeobox gene, indicates a role in the differentiation of the forebrain and the somitic mesoderm. Dev. Dyn. 210, 184–190.
Chang, C.P., Jacobs, Y., Nakamura, T., Jenkins, N.A., Copeland, N.G., Cleary, M.L., 1997. Meis proteins are major in vivo DNA binding partners for wild-type but not chimeric Pbx proteins. Mol. Cell Biol. 17, 5679–5687.
Choe, S.K., Sagerstrom, C.G., 2004. Paralog group 1 Hox genes regulate rhombomere 5/6 expression of vhnf1, a repressor of rostral hindbrain fates, in a Meis-dependent manner. Dev. Biol. 271, 350–361.
Choe, S.K., Vlachakis, N., Sagerstrom, C.G., 2002. Meis family proteins are required for hindbrain development in the Zebrafish. Development 129, 585–595.
Ebner, A., Cabernard, C., Affolter, M., Merabet, S., 2005. Recognition of distinct target sites by a unique labial/extradenticle/homothorax complex. Development 132, 1591–1600.
Ferretti, E., Marshall, H., Popperl, H., Maconochie, M., Krumlauf, R., Blasi, F., 2000. Segmental expression of Hoxb2 in r4 requires two separate sites that integrate cooperative interactions between Prep1, Pbx and Hox proteins. Development 127, 155–166.
Fire, A., Xu, S., Montgomery, M.K., Kostas, S.A., Driver, S.E., Mello, C.C., 1998. Potent and specific genetic interference by double-stranded RNA in *Caenorhabditis elegans*. Nature 391, 806–811.
Granato, M., Schnabel, H., Schnabel, R., 1994. Pha-1, a selectable marker for gene transfer in *C. Elegans*. Nucleic Acids Res. 22, 1762–1763.
Harfe, B.D., Vaz Gomes, A., Kenyon, C., Liu, J., Krause, M., Fire, A., 1998. Analysis of a *Caenorhabditis Elegans* Twist homolog identifies conserved and divergent aspects of mesodermal patterning. Genes Dev. 12, 2623–2635.
Henderson, K.D., Andrew, D.J., 2000. Regulation and function of Scr, Exd, and Hth in the *Drosophila* salivary gland. Dev. Biol. 217, 362–374.
James, P., Halladay, J., Craig, E.A., 1996. Genomic libraries and a host strain designed for highly efficient two-hybrid selection in yeast. Genetics 144, 1425–1436.
Jaw, T.J., You, L.R., Knoepfler, P.S., Yao, L.C., Pai, C.Y., Tang, C.Y., Chang, L.P., Berthelsen, J., Blasi, F., Kamps, M.P., Sun, Y.H., 2000. Direct interaction of two homeoproteins, homothorax and extradenticle, is essential for EXD nuclear localization and function. Mech. Dev. 91, 279–291.
Jiang, Y., Horner, V., Liu, J., 2005. The HMX homeodomain protein MLS-2 regulates cleavage orientation, cell proliferation and cell fate specification in the *C. Elegans* postembryonic mesoderm. Development 132, 4119–4130.
Jiang, Y., Shi, H., Amin, N.M., Sultan, I., Liu, J., 2008. Mesodermal expression of the *C. Elegans* HMX homolog Mls-2 requires the PBC homolog CEH-20. Mech. Dev. 125, 451–461.

Kamath, R.S., Fraser, A.G., Dong, Y., Poulin, G., Durbin, R., Gotta, M., Kanapin, A., Le Bot, N., Moreno, S., Sohrmann, M., Welchman, D.P., Zipperlen, P., Ahringer, J., 2003. Systematic functional analysis of the *Caenorhabditis elegans* genome using RNAi. Nature 421, 231–237.

Kelly, W.G., Xu, S., Montgomery, M.K., Fire, A., 1997. Distinct requirements for somatic and germline expression of a generally expressed *Caernorhabditis elegans* gene. Genetics 146, 227–238.

Knoepfler, P.S., Calvo, K.R., Chen, H., Antonarakis, S.E., Kamps, M.P., 1997. Meis1 and pKnox1 bind DNA cooperatively with Pbx1 utilizing an interaction surface disrupted in oncoprotein E2a-Pbx1. Proc. Natl. Acad. Sci. U. S. A. 94, 14553–14558.

Koh, K., Peyrot, S.M., Wood, C.G., Wagmaister, J.A., Maduro, M.F., Eisenmann, D.M., Rothman, J.H., 2002. Cell fates and fusion in the *C. Elegans* vulval primordium are regulated by the EGL-18 and ELT-6 GATA factors — apparent direct targets of the LIN-39 Hox protein. Development 129, 5171–5180.

Kostas, S.A., Fire, A., 2002. The T-box factor MLS-1 acts as a molecular switch during specification of nonstriated muscle in *C. elegans*. Genes Dev. 16, 257–269.

Kroon, E., Krosl, J., Thorsteinsdottir, U., Baban, S., Buchberg, A.M., Sauvageau, G., 1998. Hoxa9 transforms primary bone marrow cells through specific collaboration with Meis1a but not Pbx1b. EMBO J. 17, 3714–3725.

Krumlauf, R., 1994. Hox genes in vertebrate development. Cell 78, 191–201.

Kurant, E., Pai, C.Y., Sharf, R., Halachmi, N., Sun, Y.H., Salzberg, A., 1998. Dorsotonals/homothorax, the *Drosophila* homologue of meis1, interacts with extradenticle in patterning of the embryonic PNS. Development 125, 1037–1048.

Liu, J., Fire, A., 2000. Overlapping roles of two Hox genes and the Exd ortholog Ceh-20 in diversification of the *C. elegans* postembryonic mesoderm. Development 127, 5179–5190.

Liu, H., Strauss, T.J., Potts, M.B., Cameron, S., 2006. Direct regulation of Egl-1 and of programmed cell death by the hox protein MAB-5 and by CEH-20, a *C. elegans* homolog of Pbx1. Development 133, 641–650.

Maconochie, M.K., Nonchev, S., Studer, M., Chan, S.K., Popperl, H., Sham, M.H., Mann, R.S., Krumlauf, R., 1997. Cross-regulation in the mouse HoxB complex: the expression of Hoxb2 in rhombomere 4 is regulated by Hoxb1. Genes Dev. 11, 1885–1895.

Mann, R.S., Affolter, M., 1998. Hox proteins meet more partners. Curr. Opin. Genet. Dev. 8, 423–429.

McGinnis, W., Krumlauf, R., 1992. Homeobox genes and axial patterning. Cell 68, 283–302.

Mello, C.C., Kramer, J.M., Stinchcomb, D., Ambros, V., 1991. Efficient gene transfer in *C. elegans*: extrachromosomal maintenance and integration of transforming sequences. EMBO J. 10, 3959–3970.

Mercader, N., Tanaka, E.M., Torres, M., 2005. Proximodistal identity during vertebrate limb regeneration is regulated by Meis homeodomain proteins. Development 132, 4131–4142.

Moens, C.B., Selleri, L., 2006. Hox cofactors in vertebrate development. Dev. Biol. 291, 193–206.

Mukherjee, K., Burglin, T.R., 2007. Comprehensive analysis of animal TALE homeobox genes: new conserved motifs and cases of accelerated evolution. J. Mol. Evol. 65, 137–153.

Nagao, T., Endo, K., Kawauchi, H., Walldorf, U., Furukubo-Tokunaga, K., 2000. Patterning defects in the primary axonal scaffolds caused by the mutations of the extradenticle and homothorax genes in the embryonic *Drosophila* brain. Dev. Genes Evol. 210, 289–299.

Noro, B., Culi, J., McKay, D.J., Zhang, W., Mann, R.S., 2006. Distinct functions of homeodomain-containing and homeodomain-less isoforms encoded by homothorax. Genes Dev. 20, 1636–1650.

Pai, C.Y., Kuo, T.S., Jaw, T.J., Kurant, E., Chen, C.T., Bessarab, D.A., Salzberg, A., Sun, Y.H., 1998. The homothorax homeoprotein activates the nuclear localization of another homeoprotein, extradenticle, and suppresses eye development in *Drosophila*. Genes Dev. 12, 435–446.

Pearson, J.C., Lemons, D., McGinnis, W., 2005. Modulating Hox gene functions during animal body patterning. Nat. Rev. Genet. 6, 893–904.

Potts, M.B., Wang, D.P., Cameron, S., 2009. Trithorax, Hox, and TALE-class homeodomain proteins ensure cell survival through repression of the BH3-only gene Egl-1. Dev. Biol. 329, 374–385.

Rauskolb, C., Peifer, M., Wieschaus, E., 1993. extradenticle, a regulator of homeotic gene activity, is a homolog of the homeobox-containing human proto-oncogene pbx1. Cell 74, 1101–1112.

Rieckhof, G.E., Casares, F., Ryoo, H.D., Abu-Shaar, M., Mann, R.S., 1997. Nuclear translocation of extradenticle requires homothorax, which encodes an extradenticle-related homeodomain protein. Cell 91, 171–183.

Ryoo, H.D., Marty, T., Casares, F., Affolter, M., Mann, R.S., 1999. Regulation of Hox target genes by a DNA bound homothorax/hox/extradenticle complex. Development 126, 5137–5148.

Shanmugam, K., Green, N.C., Rambaldi, I., Saragovi, H.U., Featherstone, M.S., 1999. PBX and MEIS as non-DNA-binding partners in trimeric complexes with HOX proteins. Mol. Cell Biol. 19, 7577–7588.

Shemer, G., Podbilewicz, B., 2002. LIN-39/hox triggers cell division and represses EFF-1/fusogen-dependent vulval cell fusion. Genes Dev. 16, 3136–3141.

Shen, W.F., Rozenfeld, S., Kwong, A., Kom ves, L.G., Lawrence, H.J., Largman, C., 1999. HOXA9 forms triple complexes with PBX2 and MEIS1 in myeloid cells. Mol. Cell Biol. 19, 3051–3061.

Stevens, K.E., Mann, R.S., 2007. A balance between two nuclear localization sequences and a nuclear export sequence governs extradenticle subcellular localization. Genetics 175, 1625–1636.

Stultz, B.G., Jackson, D.G., Mortin, M.A., Yang, X., Beachy, P.A., Hursh, D.A., 2006. Transcriptional activation by extradenticle in the *Drosophila* visceral mesoderm. Dev. Biol. 290, 482–494.

Sulston, J.E., Horvitz, H.R., 1977. Post-embryonic cell lineages of the nematode, *Caenorhabditis elegans*. Dev. Biol. 56, 110–156.

Swift, G.H., Liu, Y., Rose, S.D., Bischof, L.J., Steelman, S., Buchberg, A.M., Wright, C.V., MacDonald, R.J., 1998. An endocrine–exocrine switch in the activity of the pancreatic homeodomain protein PDX1 through formation of a trimeric complex with PBX1b and MRG1 (MEIS2). Mol. Cell Biol. 18, 5109–5120.

Takacs-Vellai, K., Vellai, T., Chen, E.B., Zhang, Y., Guerry, F., Stern, M.J., Muller, F., 2007. Transcriptional control of notch signaling by a HOX and a PBX/EXD protein during vulval development in *C. elegans*. Dev. Biol. 302, 661–669.

Van Auken, K., Weaver, D., Robertson, B., Sundaram, M., Saldi, T., Edgar, L., Elling, U., Lee, M., Boese, Q., Wood, W.B., 2002. Roles of the homothorax/meis/prep homolog UNC-62 and the Exd/Pbx homologs CEH-20 and CEH-40 in *C. elegans* embryogenesis. Development 129, 5255–5268.

Wang, B.B., Müller-Immergluck, M.M., Austin, J., Robinson, N.T., Chisholm, A., Kenyon, C., 1993. A homeotic gene cluster patterns the anteroposterior body axis of *C. elegans*. Cell 74, 29–42.

Yang, L., Sym, M., Kenyon, C., 2005. The roles of two *C. elegans* HOX co-factor orthologs in cell migration and vulva development. Development 132, 1413–1428.

Zerucha, T., Prince, V.E., 2001. Cloning and developmental expression of a zebrafish meis2 homeobox gene. Mech. Dev. 102, 247–250.